Available online at www.easd.procedia.org
EASD Procedia EURODYN (2026) 302-318

EASD Procedia

EURODYN 2026
XIII International Conference on Structural Dynamics
M. Beer, C. Papadimitriou, H. Jensen, J. Chen, M. Broggi, J. Behrensdorf (eds.)
Hannover, Germany, 27.09.–01.10 2026

GREEDY LOW-RANK TENSOR APPROXIMATIONS FOR ELASTODYNAMIC GREEN'S FUNCTIONS IN LAYERED MEDIA

Z. Farooq, S. François, and G. Degrande

KU Leuven, Department of Civil Engineering
Kasteelpark Arenberg 40, B-3001 Heverlee, Belgium
e-mail: {zainab.farooq,stijn.francois,geert.degrande}@kuleuven.be

Keywords: Green's functions, Proper Generalized Decomposition, Greedy Tucker Approximation, Greedy Hierarchical Tucker Approximation, reduced order, low-rank tensor format.

Abstract. *Green's functions are fundamental ingredients in elastodynamic applications, including wave propagation and dynamic soil-structure interaction. Their numerical evaluation over dense spatial and frequency grids for multiple source-receiver configurations leads to high-dimensional Green's function tensors that impose significant computational and memory demands. To reduce these costs, the Green's functions are recasted as a separable operator represented in compact tensor form and precomputed over the parametric domain. This is achieved using tensor decomposition algorithms, including Proper Generalized Decomposition (PGD), Greedy Tucker Approximation (GTA) and Greedy Hierarchical Tucker Approximation (GHTA), introduced here as a hierarchical extension of GTA.*

The low-rank approximations are built iteratively through rank-one enrichments obtained by an alternating least-squares procedure. While PGD represents the response as a sum of separable terms, GTA couples the reduced one-dimensional spaces through a global Tucker core. GHTA extends this greedy Tucker strategy by replacing the global core with hierarchical Tucker cores arranged according to a dimension tree, providing a compact hierarchical representation of the multidimensional coupling while retaining the greedy construction of the reduced spaces. The resulting reduced Green's tensors preserve the accuracy of the reference formulation while providing compact representations that reduce storage requirements and enable efficient repeated evaluations.

Green's functions for a layered soil overlying a homogeneous halfspace are computed using PGD, GTA and GHTA, and compared with the reference direct stiffness solution. The results provide a comparative assessment of approximation accuracy, computation time, memory requirements and convergence trends.

ISSN:2311-9020 © 2026 The Authors. Published by EASD Procedia.
Peer-review under responsibility of the Organizing Committee of EURODYN 2026.
doi: 10.47964/1326.10660.180

1 INTRODUCTION

Green's functions are fundamental building blocks in computational elastodynamics, as they describe the response of an elastic medium to a unit load and underpin many formulations in wave propagation, vibration analysis and boundary element methods [1–3]. In applications such as dynamic soil-structure interaction, ground-borne vibration prediction and vibration analysis, this response is required for many combinations of source locations, receiver positions, excitation frequencies and material parameters. The resulting Green's function is therefore a multidimensional response, whose direct computation and storage can become demanding in large-scale analyses.

Model order reduction (MOR) techniques [4] have become an important tool for reducing the cost of such high-dimensional problems. Rather than evaluating and storing the full response, MOR seeks to construct a compact representation that preserves the dominant features of the high-fidelity solution. This motivates the use of MOR for Green's function computation, where the same physical problem is evaluated repeatedly for different sources, receivers, frequencies or material parameters. MOR approaches have been successfully applied to elastodynamic problems, including wave propagation [5, 6], structural vibration [7–9] and parametric analyses [10–12]. In layered soil media, reduced order representations of harmonic Green's functions have also been developed to reduce the cost of repeated evaluations [13].

Many multidimensional problems in engineering and elastodynamics can be reformulated as tensor linear systems when the governing operator and loading term admit separated representations. In such cases, the discrete problem can be written as:

$$\mathcal{A}\,\mathbf{u} = \mathcal{F} \tag{1}$$

where $\mathbf{u}$ denotes the unknown response tensor, $\mathcal{A}$ is the tensorized linear operator and $\mathcal{F}$ represents the loading term. The operator and right-hand side are then expressed as sums of tensor-product contributions involving low-dimensional operators associated with the individual coordinates or parameters. This formulation avoids the explicit construction of the full high-dimensional array and provides a suitable setting for low-rank solution algorithms.

The present work focuses on the low-rank approximation of the multidimensional Green's tensor arising from the tensorized elastodynamic problem. The multidimensional Green's tensor is not assembled or stored explicitly, instead, it is approximated using one-dimensional basis functions associated with the separable problem variables. Such low-rank representations can reduce storage requirements and improve the efficiency of repeated evaluations. Different low-rank formats arise from the way the reduced spaces associated with each variable are enriched and coupled and are discussed in this paper.

Greedy low-rank methods provide a practical way to construct such separated approximations. Proper Generalized Decomposition (PGD) [14, 15] is one of the most widely used approaches. It approximates the solution as a sum of separable rank-one terms. The approximation is built progressively by means of a greedy enrichment scheme. The resulting format is simple and storage-efficient, but strongly coupled responses may require many enrichment terms and can lead to slow convergence. The Greedy Tucker Approximation (GTA) [16] extends this strategy by enriching the reduced spaces in each dimension and computing the solution in Tucker format [17]. The coupling between these spaces is described by a core tensor, which allows different approximation ranks in the different variables. The applicability of GTA to the reduced order computation of elastodynamic Green's functions in layered soils has recently been demonstrated by the authors in [18].

A limitation of the Tucker format is that the size of the core tensor increases with both the number of dimensions and the approximation ranks. This motivates the use of hierarchical tensor formats, in which the interaction between variables is represented by a sequence of transfer tensors arranged along a dimension tree. The Greedy Hierarchical Tucker Approximation (GHTA) follows this principle by combining greedy enrichment with a hierarchical Tucker representation [19] of the reduced solution. This provides a more structured representation of multidimensional coupling than a purely rank one format, while avoiding the use of a single global Tucker core.

In this paper, PGD, GTA and GHTA are compared for the low-rank approximation of elastodynamic Green's functions in layered media. The three methods are applied to the same discretized problem, so that differences in performance can be attributed to the underlying tensor format. The GHTA formulation is part of an ongoing work on hierarchical extension of GTA and provides a first assessment of how the global Tucker core can be replaced by a structured hierarchy of coupling tensors. The comparison considers approximation accuracy, computational cost and storage requirements, with the aim of assessing the suitability of these formats for reduced order Green's function modelling in elastodynamics.

2 ELASTODYNAMIC GREEN'S FUNCTIONS

This work considers two-dimensional wave propagation in the (x, z)-plane in a horizontally layered soil medium overlying a homogeneous halfspace. For this class of problems, the elastodynamic response separates into in-plane P-SV motion and out-of-plane SH motion. The formulation is introduced in the frequency domain and transformed in the horizontal direction by exploiting the invariance of the medium along x.

A horizontally layered soil domain Ω_{S} of infinite horizontal extent is considered, as shown in figure 1. The medium is subjected to a concentrated pulse load $\rho\hat{\mathbf{b}}(\mathbf{x}, \omega) = \delta(\mathbf{x} - \mathbf{x}_{\mathrm{s}})\mathbf{e}_i$ applied at location $\mathbf{x}_{\mathrm{s}}$ in direction $\mathbf{e}_i$. $\rho\hat{\mathbf{b}}$ represents body forces, ρ is the material density, ω is the excitation frequency and $\delta(\cdot)$ denotes the Dirac delta function. A hat above a variable denotes its representation in the frequency domain.

The corresponding displacement field $\hat{\mathbf{u}}(\mathbf{x}, \omega)$ evaluated at location $\mathbf{x}$ is called a Green's function or fundamental solution of the layered soil domain. In the frequency domain, the elastodynamic equilibrium equation is expressed as:

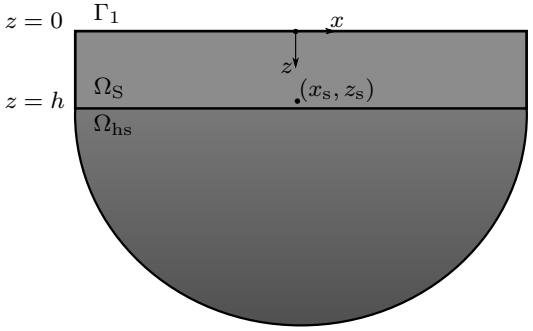

Figure 1: Horizontally layered soil medium overlying a homogeneous halfspace. A concentrated pulse load $\rho\hat{\mathbf{b}}(\mathbf{x}, \omega) = \delta(x)\delta(z - z_{\mathrm{s}})\mathbf{e}_i$ is applied at $\mathbf{x}_{\mathrm{s}} = \{0,\ z_{\mathrm{s}}\}^{\mathrm{T}}$ in direction $\mathbf{e}_i$.

$$\mathbf{L}^{\mathrm{T}}\hat{\boldsymbol{\sigma}} + \rho\hat{\mathbf{b}} = -\rho\omega^2\hat{\mathbf{u}} \quad \text{in} \quad \Omega_{\mathrm{S}} \tag{2}$$

where $\hat{\boldsymbol{\sigma}}$ denotes the stress vector and $\mathbf{L}$ the differential operator. Their forms depend on whether the P-SV or SH wave motion is considered.

Using a weighted residual formulation and exploiting the horizontal invariance of the medium, the coordinate x is transformed to the wavenumber domain k_x, or equivalently to the slowness variable $p_x = k_x/\omega$. The transformed formulation describes the vertical dependence through the thin layer discretization and accounts for the underlying homogeneous halfspace through a dynamic impedance matrix [20]. The Green's function then remains parametrized by the source position, source depth, horizontal slowness and receiver depth. This structure provides the basis for defining the multidimensional Green's tensor considered for low-rank approximation in the following sections. The complete derivation of the governing equations and weak formulation of the layered halfspace model is provided in [18].

3 LOW-RANK APPROXIMATION OF GREEN'S FUNCTIONS

The reduced order representation is constructed based on the low-rank structure of the Green's function in the wavenumber domain. For a fixed excitation frequency ω, the Green's function $\tilde{\mathbf{u}}^{\mathrm{G}}(x_{\mathrm{s}}, z_{\mathrm{s}}, p_x, z; \omega)$ is approximated with respect to four problem variables, the source position x_{s}, the source depth z_{s}, the horizontal slowness p_x and the receiver depth z. The aim is to replace the full multidimensional response by a compact low-rank representation that reduces storage requirements and facilitates repeated evaluations.

In this work, three greedy tensor-based approaches are considered for this purpose, namely PGD [14, 15], GTA [16] and GHTA, introduced here as a hierarchical extension of the greedy Tucker strategy. GHTA replaces the global Tucker core by a hierarchical Tucker (HT) representation [19] based on a dimension tree, its detailed formulation is presented in subsection 3.3. All these methods are used as algebraic low-rank solvers for the tensorized problem and provide an a priori model reduction of the Green's function, primarily differing in the tensor structure used to represent the reduced solution.

3.1 Proper Generalized Decomposition

Proper Generalized Decomposition (PGD) is a greedy rank-one method for constructing separated approximations of high-dimensional problems [14, 15]. The solution is built progressively as a sum of separable contributions, each expressed as the outer product of one-dimensional functions. From a tensor perspective, this representation corresponds to a Canonical Polyadic Decomposition (CPD) [17]. For the present four-dimensional problem, the Green's displacement tensor is approximated as:

$$\tilde{\mathbf{u}}^{\mathrm{G}}(x_{\mathrm{s}}, z_{\mathrm{s}}, p_x, z; \omega) \approx \boldsymbol{\mathcal{U}} = \sum_{r=1}^{R_u} \mathbf{u}_r^{\mathrm{G}(x_{\mathrm{s}})}(x_{\mathrm{s}}) \otimes \mathbf{u}_r^{\mathrm{G}(z_{\mathrm{s}})}(z_{\mathrm{s}}) \otimes \mathbf{u}_r^{\mathrm{G}(p_x)}(p_x) \otimes \mathbf{u}_r^{\mathrm{G}(z)}(z) \tag{3}$$

where R_u denotes the number of rank-one enrichment terms. The functions $\mathbf{u}_r^{\mathrm{G}(x_{\mathrm{s}})}(x_{\mathrm{s}})$, $\mathbf{u}_r^{\mathrm{G}(z_{\mathrm{s}})}(z_{\mathrm{s}})$, $\mathbf{u}_r^{\mathrm{G}(p_x)}(p_x)$ and $\mathbf{u}_r^{\mathrm{G}(z)}(z)$ are defined on corresponding one-dimensional domains, $x_{\mathrm{s}} \in \mathcal{I}_{x_{\mathrm{s}}}$, $z_{\mathrm{s}} \in \mathcal{I}_{z_{\mathrm{s}}}$, $p_x \in \mathcal{I}_{p_x}$ and $z \in \mathcal{I}_z$, respectively.

The approximation is constructed sequentially through greedy enrichments. At enrichment step $R_u + 1$, a new separable correction is computed in the form:

$$\boldsymbol{\mathcal{U}}_{R_u+1} = \underline{\mathbf{u}}_{R_u+1}^{(x_{\mathrm{s}})} \otimes \underline{\mathbf{u}}_{R_u+1}^{(z_{\mathrm{s}})} \otimes \underline{\mathbf{u}}_{R_u+1}^{(p_x)} \otimes \underline{\mathbf{u}}_{R_u+1}^{(z)} \tag{4}$$

The one-dimensional factors are obtained from the tensorized linear system by enforcing a residual orthogonality condition for the current enrichment. The resulting problem is nonlinear with respect to the unknown factors, since the separated functions appear as products. It is therefore solved by an alternating least-squares (ALS) procedure, in which one factor is updated at a time while the others are kept fixed. The alternating iterations are continued until convergence of the enrichment term. After convergence, the new rank-one correction is added to the current approximation and the residual is updated. The greedy procedure is repeated until the prescribed tolerance is reached or the maximum number of enrichment terms is attained. In general, increasing R_u improves the approximation accuracy.

The main limitation of PGD is that strongly coupled responses may require many separable rank-one contributions. Since each enrichment is fully separable, interactions between the problem variables are captured only through the accumulation of successive rank-one contributions. For Green's functions with strong multidimensional coupling, this can lead to slow convergence and residual stagnation. In such cases, increasing the number of enrichments does not provide an efficient reduction of the approximation error. This motivates the use of Tucker and hierarchical Tucker formats, where the reduced spaces are coupled more flexibly.

3.2 Greedy Tucker Approximation

The Greedy Tucker Approximation (GTA) extends the PGD enrichment strategy by constructing reduced spaces in each separated direction and representing their coupling through a Tucker core. As in PGD, the reduced spaces are built progressively from rank-one enrichments computed by an ALS procedure. After each enrichment, the newly obtained mode-wise functions are orthonormalized and appended to the corresponding one-dimensional bases. The tensorized system is then projected onto the tensor product space generated by these bases and the reduced problem is solved for the core coefficients. The resulting approximation therefore combines greedily constructed one-dimensional spaces with a global core tensor that accounts for their multidimensional coupling, without requiring explicit assembly of the full Green's function tensor.

For the present problem, the Green's displacement tensor is approximated as:

$$\tilde{\mathbf{u}}^{\mathrm{G}}(x_{\mathrm{s}}, z_{\mathrm{s}}, p_x, z; \omega) \approx \boldsymbol{\mathcal{U}} = \sum_{r_{x_{\mathrm{s}}}=1}^{R_{x_{\mathrm{s}}}} \sum_{r_{z_{\mathrm{s}}}=1}^{R_{z_{\mathrm{s}}}} \sum_{r_{p_x}=1}^{R_{p_x}} \sum_{r_z=1}^{R_z} g_{r_{x_{\mathrm{s}}} r_{z_{\mathrm{s}}} r_{p_x} r_z} \mathbf{u}_{r_{x_{\mathrm{s}}}}^{\mathrm{G}(x_{\mathrm{s}})}(x_{\mathrm{s}}) \otimes \mathbf{u}_{r_{z_{\mathrm{s}}}}^{\mathrm{G}(z_{\mathrm{s}})}(z_{\mathrm{s}}) \otimes \mathbf{u}_{r_{p_x}}^{\mathrm{G}(p_x)}(p_x) \otimes \mathbf{u}_{r_z}^{\mathrm{G}(z)}(z) \quad (5)$$

where $R_{x_{\mathrm{s}}}, R_{z_{\mathrm{s}}}, R_{p_x}$ and R_z denote the Tucker ranks associated with the four approximation dimensions. The coefficient $g_{r_{x_{\mathrm{s}}} r_{z_{\mathrm{s}}} r_{p_x} r_z}$ belongs to the Tucker core tensor and describes the coupling between the one-dimensional basis functions. The functions $\mathbf{u}_{r_{x_{\mathrm{s}}}}^{\mathrm{G}(x_{\mathrm{s}})}(x_{\mathrm{s}})$, $\mathbf{u}_{r_{z_{\mathrm{s}}}}^{\mathrm{G}(z_{\mathrm{s}})}(z_{\mathrm{s}})$, $\mathbf{u}_{r_{p_x}}^{\mathrm{G}(p_x)}(p_x)$ and $\mathbf{u}_{r_z}^{\mathrm{G}(z)}(z)$ are defined on their respective one-dimensional domains, $x_{\mathrm{s}} \in \mathcal{I}_{x_{\mathrm{s}}}$, $z_{\mathrm{s}} \in \mathcal{I}_{z_{\mathrm{s}}}$, $p_x \in \mathcal{I}_{p_x}$ and $z \in \mathcal{I}_z$. The multilinear ranks determine the size of the reduced spaces in the Tucker representation. As these ranks increase, the approximation accuracy generally improves. Compared with PGD, GTA provides richer representation by coupling the one-dimensional reduced spaces through the Tucker core. This allows the reduced basis functions in different dimensions to interact directly, rather than only through the accumulation of rank-one terms. For Green's functions in layered media, this is important because the response may depend in a coupled way on the source position, source depth, slowness and receiver depth.

The applicability of GTA to the reduced order modelling of elastodynamic Green's functions in layered soils has been demonstrated in [18].

A limitation of the Tucker format is the growth of the core tensor. Since the core size scales with the product of the multilinear ranks, the storage requirements and computational cost may increase significantly as the ranks grow. For the present four-dimensional approximation, the number of core coefficients is $R_{x_s} R_{z_s} R_{p_x} R_z$. This scaling becomes more restrictive when additional spatial, spectral, or material parameters are introduced. This motivates the use of hierarchical tensor formats, which aim to retain a coupled representation of the reduced spaces while avoiding the use of a single global Tucker core.

3.3 Greedy Hierarchical Tucker Approximation

The Greedy Hierarchical Tucker Approximation (GHTA) extends the greedy Tucker strategy by representing the reduced solution in HT format. The aim is to retain the coupled representation of the reduced spaces, as in GTA, while avoiding the use of a single global Tucker core. Instead, the coupling between variables is described through a hierarchy of smaller core tensors arranged according to a dimension tree.

The dimension tree defines how the variables are grouped in the hierarchical representation. The root node contains the complete set of variables, the leaf nodes correspond to the individual variables and each internal node represents the union of two child subsets. At the leaf level, basis matrices are associated with the one-dimensional reduced spaces generated by the greedy enrichment procedure. At the internal nodes, transfer tensors combine the bases of the child nodes and define reduced bases for the corresponding parent subsets. The multidimensional approximation is therefore built recursively from the leaves to the root.

In contrast to GTA, where all reduced spaces are coupled through a single Tucker core, GHTA distributes this coupling over the internal nodes of the dimension tree. This reduces the dependence on one global core tensor and provides a more scalable representation when the number of dimensions or the required ranks increase.

3.3.1 Hierarchical representation of Green's functions

For the present problem, two dimension tree configurations are considered. In the first configuration, the variables are grouped according to the tree shown in figure 2, where the source coordinates $(x_\mathrm{s}, z_\mathrm{s})$ form the first branch and the slowness-receiver coordinates (p_x, z) form the second branch. For this tree structure, the Tucker core tensor is replaced by the hierarchical transfer tensors $\boldsymbol{\mathcal{B}}^{(x_\mathrm{s},z_\mathrm{s})}$, $\boldsymbol{\mathcal{B}}^{(p_x,z)}$ and $\boldsymbol{\mathcal{B}}^{(x_\mathrm{s},(z_\mathrm{s},(p_x,z)))}$, which describe the couplings within each branch and between both branches at the root level.

An alternative hierarchical representation is considered using the dimension tree shown in figure 3. In this configuration, the source position x_s is separated at the root level, while the remaining variables are grouped in the branch $(z_\mathrm{s}, (p_x, z))$. The source depth z_s is then coupled with the slowness-receiver branch (p_x, z), where the horizontal slowness p_x and receiver depth z form the lowest-level branch. For this tree structure, the global Tucker core is replaced by the hierarchical transfer tensors $\boldsymbol{\mathcal{B}}^{(p_x,z)}$, $\boldsymbol{\mathcal{B}}^{(z_\mathrm{s},(p_x,z))}$ and $\boldsymbol{\mathcal{B}}^{(x_\mathrm{s},(z_\mathrm{s},(p_x,z)))}$. The core $\boldsymbol{\mathcal{B}}^{(p_x,z)}$ describes the coupling between the horizontal slowness and receiver depth, while $\boldsymbol{\mathcal{B}}^{(z_\mathrm{s},(p_x,z))}$ couples the source-depth basis with the reduced representation of the (p_x, z) branch. The root core $\boldsymbol{\mathcal{B}}^{(x_\mathrm{s},(z_\mathrm{s},(p_x,z)))}$ couples the source position (x_s) basis with the reduced representation of the branch $(z_\mathrm{s}, (p_x, z))$. The remainder of the paper adopts the second dimension tree configuration, which provided improved convergence for the considered Green's function approximation. For

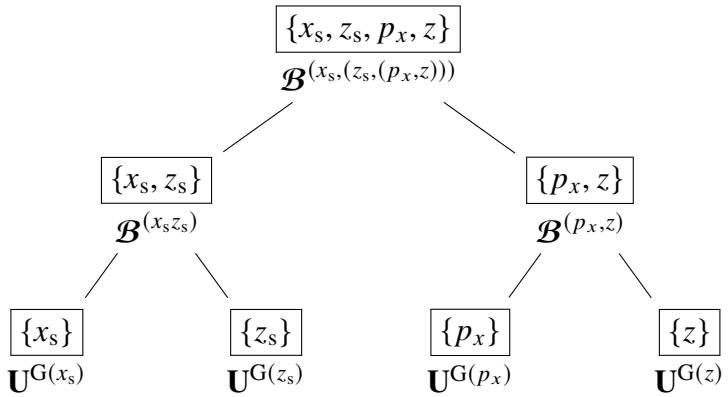

Figure 2: Dimension tree configuration 1.

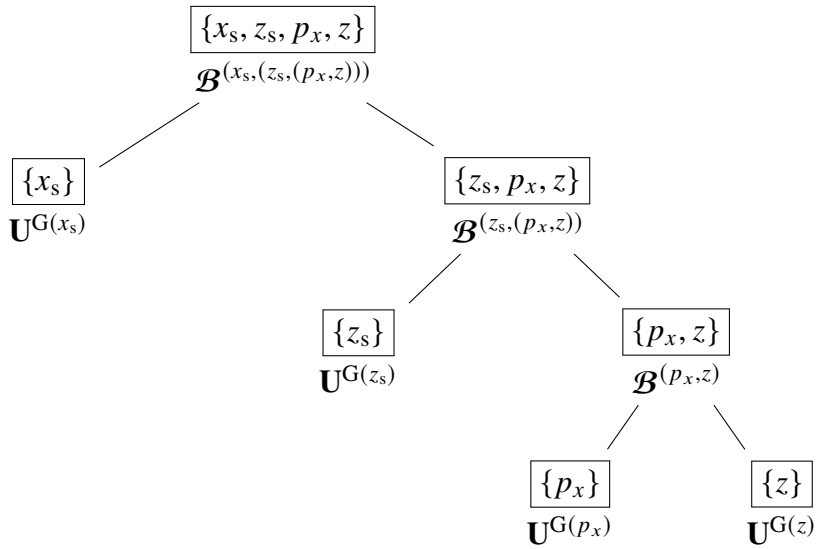

Figure 3: Dimension tree configuration 2.

the numerical implementation, these hierarchicial core tensors are computed in matricized form and subsequently reshaped into their tensor representation.

$$\begin{aligned}
\mathbf{B}^{(p_x,z)} &\in \mathbb{R}^{(R_{p_x} R_z)\times R_{p_x z}} \quad \Longrightarrow \quad \mathcal{B}^{(p_x,z)} \quad \in \mathbb{R}^{R_{p_x}\times R_z \times R_{p_x z}} \\
\mathbf{B}^{(z_s,(p_x,z))} &\in \mathbb{R}^{(R_{z_s} R_{p_x z})\times R_{z_s p_x z}} \quad \Longrightarrow \quad \mathcal{B}^{(z_s,(p_x,z))} \quad \in \mathbb{R}^{R_{z_s}\times R_{p_x z}\times R_{z_s p_x z}} \\
\mathbf{B}^{(x_s,(z_s,(p_x,z)))} &\in \mathbb{R}^{(R_{x_s} R_{z_s p_x z})\times 1} \quad \Longrightarrow \quad \mathcal{B}^{(x_s,(z_s,(p_x,z)))} \in \mathbb{R}^{R_{x_s}\times R_{z_s p_x z}\times 1}
\end{aligned} \tag{6}$$

Based on the adopted dimension tree, the Green's displacement tensor can be represented in hierarchical Tucker form by first combining the leaf factor matrices of the lowest-level branch (p_x, z), then coupling this branch with the source depth basis z_s and finally coupling the resulting representation with the source position x_s basis at the root level. The hierarchical modes associated with the slowness-receiver branch (p_x, z) are given by:

$$\tilde{\mathbf{u}}^{G(p_x,z)}_{r_{p_x z}} = \sum_{r_{p_x}=1}^{R_{p_x}} \sum_{r_z=1}^{R_z} b^{(p_x,z)}_{r_{p_x} r_z r_{p_x z}} \, \mathbf{u}^{G(p_x)}_{r_{p_x}}(p_x) \otimes \mathbf{u}^{G(z)}_{r_z}(z) \tag{7}$$

This branch is then coupled with the source depth basis to define the hierarchical modes

associated with $(z_\mathrm{s}, (p_x, z))$:

$$\tilde{\mathbf{u}}^{\mathrm{G}(z_\mathrm{s},(p_x,z))}_{r_{z_\mathrm{s}} p_x z} = \sum_{r_{z_\mathrm{s}}=1}^{R_{z_\mathrm{s}}} \sum_{r_{p_x z}=1}^{R_{p_x z}} b^{(z_\mathrm{s},(p_x,z))}_{r_{z_\mathrm{s}} r_{p_x z} r_{z_\mathrm{s} p_x z}} \mathbf{u}^{\mathrm{G}(z_\mathrm{s})}_{r_{z_\mathrm{s}}}(z_\mathrm{s}) \otimes \mathbf{u}^{\mathrm{G}(p_x,z)}_{r_{p_x z}} \tag{8}$$

The Green's displacement tensor is finally obtained by coupling the source-position basis with the reduced representation of the branch $(z_\mathrm{s}, (p_x, z))$ through the root tensor $\boldsymbol{\mathcal{B}}^{(x_\mathrm{s},(z_\mathrm{s},(p_x,z)))}$:

$$\tilde{\mathbf{u}}^{\mathrm{G}}(x_\mathrm{s}, z_\mathrm{s}, p_x, z; \omega) \approx \sum_{r_{x_\mathrm{s}}=1}^{R_{x_\mathrm{s}}} \sum_{r_{z_\mathrm{s} p_x z}=1}^{R_{z_\mathrm{s} p_x z}} b^{(x_\mathrm{s},(z_\mathrm{s},(p_x,z)))}_{r_{x_\mathrm{s}} r_{z_\mathrm{s} p_x z}} \mathbf{u}^{\mathrm{G}(x_\mathrm{s})}_{r_{x_\mathrm{s}}}(x_\mathrm{s}) \otimes \mathbf{u}^{\mathrm{G}(z_\mathrm{s},(p_x,z))}_{r_{z_\mathrm{s} p_x z}} \tag{9}$$

3.3.2 Computation of the hierarchical Tucker representation

The GHTA formulation retains the greedy enrichment scheme used to construct the one-dimensional reduced spaces associated with x_s, z_s, p_x and z. Its main distinction from PGD and GTA lies in how the coupling between these spaces is represented. In PGD, the enrichment functions are accumulated as separable rank-one terms, whereas in GTA the reduced spaces are coupled through a single Tucker core. In GHTA, this coupling is represented by hierarchical Tucker cores arranged according to the selected dimension tree.

After each greedy enrichment, the one-dimensional reduced spaces are updated and kept fixed while the hierarchical Tucker cores are recomputed. For these fixed leaf bases, the remaining unknowns are the root core and the transfer cores associated with the internal nodes of the tree. These cores define the coupling between the reduced spaces and determine the hierarchical approximation of the Green's function. For the dimension tree (figure 3), the hierarchical approximation depends on the root core $\boldsymbol{\mathcal{B}}^{(x_\mathrm{s},(z_\mathrm{s},(p_x,z)))}$ and the transfer cores $\boldsymbol{\mathcal{B}}^{(z_\mathrm{s},(p_x,z))}$ and $\boldsymbol{\mathcal{B}}^{(p_x,z)}$. For the current leaf bases, the separated operators and right-hand side terms are first projected onto the reduced spaces. The residual associated with the current reduced hierarchical approximation is then written as:

$$\boldsymbol{\mathcal{R}}_{\mathrm{HT}} = \bar{\boldsymbol{\mathcal{F}}} - \bar{\boldsymbol{\mathcal{A}}}\, \boldsymbol{\mathcal{U}}_{\mathrm{HT}} \left(\boldsymbol{\mathcal{B}}^{(x_\mathrm{s},(z_\mathrm{s},(p_x,z)))}, \boldsymbol{\mathcal{B}}^{(z_\mathrm{s},(p_x,z))}, \boldsymbol{\mathcal{B}}^{(p_x,z)} \right) \tag{10}$$

where $\boldsymbol{\mathcal{U}}_{\mathrm{HT}}$ denotes the hierarchical Tucker approximation constructed from the current leaf bases and HT cores. The assembly of the hierarchical representation is done using the htucker toolbox [19]. The quantities $\bar{\boldsymbol{\mathcal{A}}}$ and $\bar{\boldsymbol{\mathcal{F}}}$ denote the projected tensorized operator and right-hand side, respectively. For each separated operator term $r_a = 1, \ldots, R_a$, the projected one-dimensional operators are given by:

$$\bar{\mathbf{A}}^{(\theta)}_{r_a} = \left(\mathbf{U}^{\mathrm{G}(\theta)} \right)^{\mathrm{T}} \mathbf{A}^{(\theta)}_{r_a} \mathbf{U}^{\mathrm{G}(\theta)}, \qquad \theta \in \{x_\mathrm{s}, z_\mathrm{s}, p_x, z\} \tag{11}$$

The projected tensorized operator is then assembled as:

$$\bar{\boldsymbol{\mathcal{A}}} = \sum_{r_a=1}^{R_a} \bar{\mathbf{A}}^{(x_\mathrm{s})}_{r_a} \otimes \bar{\mathbf{A}}^{(z_\mathrm{s})}_{r_a} \otimes \bar{\mathbf{A}}^{(p_x)}_{r_a} \otimes \bar{\mathbf{A}}^{(z)}_{r_a} \tag{12}$$

Similarly, for each separated right-hand side term $r_f = 1, \ldots, R_f$, the reduced load factors are:

$$\bar{\mathbf{F}}^{(\theta)}_{r_f} = \left(\mathbf{U}^{\mathrm{G}(\theta)} \right)^{\mathrm{T}} \mathbf{F}^{(\theta)}_{r_f}, \qquad \theta \in \{x_\mathrm{s}, z_\mathrm{s}, p_x, z\} \tag{13}$$

and the projected right-hand side is assembled as:

$$\bar{\mathcal{F}} = \sum_{r_f=1}^{R_f} \bar{\mathbf{F}}_{r_f}^{(x_s)} \otimes \bar{\mathbf{F}}_{r_f}^{(z_s)} \otimes \bar{\mathbf{F}}_{r_f}^{(p_x)} \otimes \bar{\mathbf{F}}_{r_f}^{(z)} \tag{14}$$

Since the hierarchical approximation depends multilinearly on the HT cores, the reduced core problem is solved using an ALS procedure. At each core iteration, the HT cores associated with the internal nodes of the dimension tree are updated successively, while the remaining cores are kept fixed. This makes the residual equation linear with respect to the unknown entries of the core being updated, leading to a reduced least-squares problem for that core. After each ALS iteration, the hierarchical approximation is reconstructed and the reduced residual is evaluated. The HT transfer cores are orthonormalized to improve the conditioning of subsequent ALS updates. The resulting HT cores define the hierarchical Tucker representation of the Green's function at the current greedy enrichment level.

4 NUMERICAL EXAMPLE

This section illustrates the application of the reduced order algorithms to the low-rank approximation of Green's functions for a layered soil problem.

4.1 Problem outline

A soil layer overlying a homogeneous halfspace is considered (figure 1). The corresponding soil and halfspace properties are summarized in table 1. The soil layer is modeled using thin layer matrices, while the halfspace contribution is represented analytically using an impedance relation linking displacements and tractions at the interface [20]. This impedance term is appended to the dynamic stiffness matrix of the layered system, as detailed in [18]. Material damping is assumed to be hysteretic and rate-independent. According to the correspondence principle, the complex Lamé constants are defined as $\mu^\star = \mu(1 + 2\beta_\mathrm{s}\mathrm{i})$ and $(\lambda^\star + 2\mu^\star) = (\lambda + 2\mu)(1 + 2\beta_\mathrm{p}\mathrm{i})$ [21].

Table 1: Soil properties for the numerical example.

Soil profile	h [m]	C_s [m/s]	C_p [m/s]	β_s [-]	β_p [-]	ρ [kg/m^3]
Soil layer	10	100	300	0.020	0.020	1800
Homogeneous halfspace	∞	260	1726	0.020	0.020	1970

The model coordinates comprise the source position x_s, source depth z_s, receiver depth z and slowness p_x at a fixed frequency ω. The analysis is carried out for SH and P-SV wave propagation. The Green's displacements in the wavenumber–frequency domain solution are computed using the direct stiffness method [20, 22] and are referred to as the full order model (FOM). The displacements are then approximated using PGD, GTA [18] and GHTA and the resulting reduced order solutions are compared with the FOM. To improve efficiency, the wavenumber domain is parametrized in terms of slowness. Multiplying the slowness p_x with the shear wave velocity C_s yields the dimensionless wavenumber $\bar{k}_x = k_x C_\mathrm{s}/\omega = p_x C_\mathrm{s}$. The wavenumber domain is sampled logarithmically using 1200 points, with positive and negative values distributed symmetrically over $|k_x| \in [10^{-2}, 10^{2}]$. The source position is sampled as

$x_s \in [-5, 5]$ m using 100 uniformly distributed points, while the source depth is sampled as $z_s \in [0, 10]$ m with a spacing of 0.10 m. The receiver depths correspond to the vertical coordinates of the thin layer mesh. To enable the subsequent evaluation of the spatial–frequency response, the horizontal receiver coordinate is sampled over the interval $x \in [-60, 60]$ m using 400 uniformly distributed points.

GHTA constructs the reduced spaces through successive greedy enrichments along the tensor dimensions, followed by the computation of the HT core tensors in the reduced space. The enrichment iterations are performed using a Petrov-Galerkin formulation [15]. The greedy procedure is stopped when the prescribed tolerance of 10^{-5} is reached or when the maximum number of 15 enrichment modes is attained. The same tolerance and maximum number of modes are used for PGD and GTA to ensure a consistent comparison between the three methods.

4.2 SH Green's functions

Results are first presented for the SH Green's function. For SH wave propagation, the motion is purely out-of-plane and the in-plane displacement components $\hat{u}_x$ and $\hat{u}_z$ are zero. The displacement vector reduces to $\hat{\mathbf{u}} = \{\hat{u}_y\}^{\mathrm{T}}$. In this case, only the shear strains remain non-zero, reducing the strain vector to $\hat{\boldsymbol{\epsilon}} = \{\hat{\gamma}_{xy}, \hat{\gamma}_{zy}\}^{\mathrm{T}}$. The corresponding stress vector becomes $\hat{\boldsymbol{\sigma}} = \{\hat{\sigma}_{xy}, \hat{\sigma}_{zy}\}^{\mathrm{T}}$. Figure 4a presents the SH Green's displacement component $\tilde{u}^{\mathrm{G}}_{yy}(x_s, z_s, p_x, z)$ at the soil surface ($z = 0\,\mathrm{m}$) in the wavenumber-frequency domain at $f = 5\,\mathrm{Hz}$ due to a concentrated load applied at $x_s = 0\,\mathrm{m}$ and $z_s = 0\,\mathrm{m}$. The corresponding wavefield $\hat{u}^{\mathrm{G}}_{yy}(x_s, z_s, x, z)$ in the spatial domain is obtained by applying the inverse logarithmic Fourier transform [22, 23] to the wavenumber-frequency solution and is shown in figure 5 for FOM and reduced algorithms.

The low-rank structure of the decomposition allows this transformation to be carried out directly on the relevant factor matrix, i.e. $\mathbf{u}^{\mathrm{G}(p_x)}_{r_{p_x}}(p_x)$, rather than on the full Green's tensor. In a conventional full-grid transformation, the inverse transform must be carried out over the complete discretized tensor of size $n(x_s) \times n(z_s) \times n(p_x) \times n(z)$, where $n(x_s)$ and $n(z_s)$ denote the number of source positions, $n(p_x)$ the number of slowness samples and $n(z)$ the number of vertical discretization points. In contrast, the reduced representation requires the transformation only of the reduced basis associated with slowness $\mathbf{u}^{\mathrm{G}(p_x)}_{r_{p_x}}(p_x)$. The spatial response (figure 4b) at $z = 0\,\mathrm{m}$ and $f = 5\,\mathrm{Hz}$ exhibits an oscillatory pattern with a wavelength of approximately 20 m, corresponding to the shear wavelength. The response is largest near the source and decreases

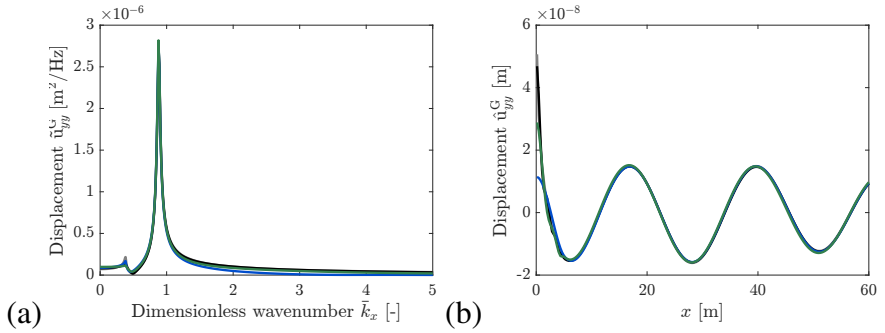

Figure 4: SH Green's displacement (a) $\tilde{u}^{\mathrm{G}}_{yy}(x_s, z_s, p_x, z)$ as a function of dimensionless wavenumber and (b) $\hat{u}^{\mathrm{G}}_{yy}(x_s, z_s, x, z)$ as a function of x, evaluated at $z = 0\,\mathrm{m}$ and $f = 5\,\mathrm{Hz}$ for an out-of-plane concentrated load applied at $x_s = 0\,\mathrm{m}$ and $z_s = 0\,\mathrm{m}$ using FOM (gray), PGD (blue), GTA (black) and GHTA (green).

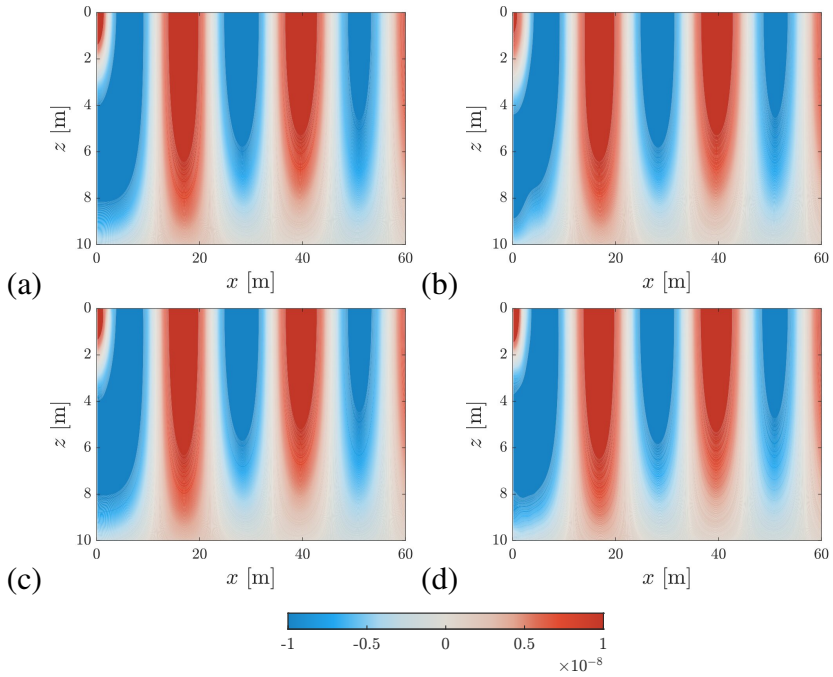

Figure 5: SH Green's displacement $\hat{u}^{\mathrm{G}}_{yy}(x_{\mathrm{s}}, z_{\mathrm{s}}, x, z)$ computed at $f = 5\,\mathrm{Hz}$ for an out-of-plane concentrated load applied at $x_{\mathrm{s}} = 0\,\mathrm{m}$ and $z_{\mathrm{s}} = 0\,\mathrm{m}$ using (a) FOM, (b) PGD, (c) GTA and (d) GHTA.

with distance depending upon the material damping.

For the SH problem, all reduced order models reproduce the main features of the FOM response with reasonable accuracy. For 15 enrichment modes, the GTA approximation provides the closest agreement with the FOM response, whereas PGD shows the largest discrepancy. This trend is consistent with the underlying approximation formats. PGD is restricted to an accumulation of fully separable rank-one terms, while GTA couples all reduced spaces through a global Tucker core. GHTA gives an intermediate approximation, as the hierarchical Tucker representation introduces coupling through the dimension tree without retaining the full global coupling of the Tucker core.

4.3 P-SV Green's functions

The low-rank approximation is further assessed for the P-SV Green's functions of the layered medium. The P-SV problem involves in-plane wave propagation, for which the out-of-plane displacement component $\hat{u}_y$ vanishes and the displacement vector reduces to $\hat{\mathbf{u}} = \{\hat{u}_x, \hat{u}_z\}^{\mathrm{T}}$. All variables are independent of the coordinate y, resulting in $\hat{\epsilon}_{yy} = \hat{\gamma}_{xy} = \hat{\gamma}_{yz} = 0$. The remaining strain and stress components are collected as $\hat{\boldsymbol{\epsilon}} = \{\hat{\epsilon}_{xx}, \hat{\epsilon}_{zz}, \hat{\gamma}_{zx}\}^{\mathrm{T}}$ and $\hat{\boldsymbol{\sigma}} = \{\hat{\sigma}_{xx}, \hat{\sigma}_{zz}, \hat{\sigma}_{zx}\}^{\mathrm{T}}$. Consequently, the elastodynamic Green's displacement is vector-valued and represents the horizontal and vertical response of the medium to in-plane point loads. In matrix form, the P-SV Green's displacement is expressed as:

$$\hat{\mathbf{u}}^{\mathrm{G}} = \begin{bmatrix} \hat{u}^{\mathrm{G}}_{xx} & \hat{u}^{\mathrm{G}}_{zx} \\ \hat{u}^{\mathrm{G}}_{xz} & \hat{u}^{\mathrm{G}}_{zz} \end{bmatrix} \tag{15}$$

These four components describe both co-directional and cross-directional responses and together characterize the coupled propagation of compressional and shear waves in the medium. In the

present comparison, the component $\tilde{u}^{\mathrm{G}}_{zz}$ is selected as a representative P-SV response. This component corresponds to the vertical displacement induced by a vertical unit load on the layered medium.

Figure 6a presents the P-SV Green's displacement component $\tilde{u}^{\mathrm{G}}_{zz}(x_{\mathrm{s}}, z_{\mathrm{s}}, p_x, z)$ in the wavenumber domain at $f = 5$ Hz. The corresponding spatial wavefield, obtained by inverse transformation of the wavenumber-domain response, is shown in figure 7. The spatial response (figure 6b) at $z = 0$ m and $f = 5$ Hz exhibits an oscillatory pattern with a wavelength of approximately 19 m, corresponding to the Rayleigh wavelength [24]. The response is largest near the source and decreases with distance depending upon the material damping. Compared with the SH case, the P-SV problem is more demanding because the response involves coupled displacement components and stronger modal interactions. For the prescribed maximum of 16 enrichment modes, the reduced order approximations remain challenging. The GTA approximation is limited by the memory growth of the Tucker core, while the PGD approximation becomes numerically unstable. The current GHTA approximation provides a feasible hierarchical representation, although its accuracy remains sensitive to the selected internal ranks and dimension tree.

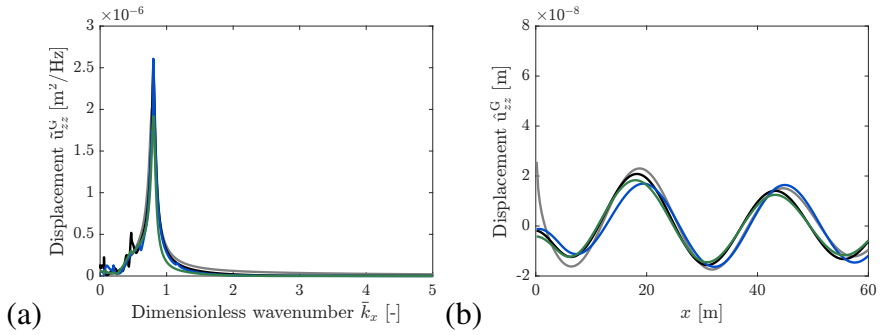

Figure 6: P-SV Green's displacement (a) $\tilde{u}^{\mathrm{G}}_{zz}(x_{\mathrm{s}}, z_{\mathrm{s}}, p_x, z)$ as a function of dimensionless wavenumber and (b) $\hat{u}^{\mathrm{G}}_{zz}(x_{\mathrm{s}}, z_{\mathrm{s}}, x, z)$ as a function of x, evaluated at $z = 0$ m and $f = 5$ Hz for an out-of-plane concentrated load applied at $x_{\mathrm{s}} = 0$ m and $z_{\mathrm{s}} = 0$ m using FOM(gray), PGD (blue), GTA (black) and GHTA (green).

4.4 Performance comparison of reduced order algorithms

The performance of the reduced order algorithms is assessed by comparing the PGD, GTA and GHTA approximations with the reference FOM solution. The comparison is carried out in terms of approximation accuracy, convergence with respect to the number of enrichment modes, computational cost and storage requirements.

The computation times of the FOM and reduced order approximations are summarized in the table 2. For the FOM, the reported time corresponds to the direct computation of the Green's tensor. For PGD, GTA and GHTA, the offline time corresponds to the construction of the low-rank representation, while the online time corresponds to the reassembly or evaluation of the Green's function from the stored reduced factors. The offline stage requires a higher computational cost than a single FOM evaluation, since the reduced bases and coupling coefficients are built iteratively through greedy enrichment. Once constructed, however, the reduced representations can be evaluated efficiently through low-rank tensor contractions, without recomputing the full Green's tensor.

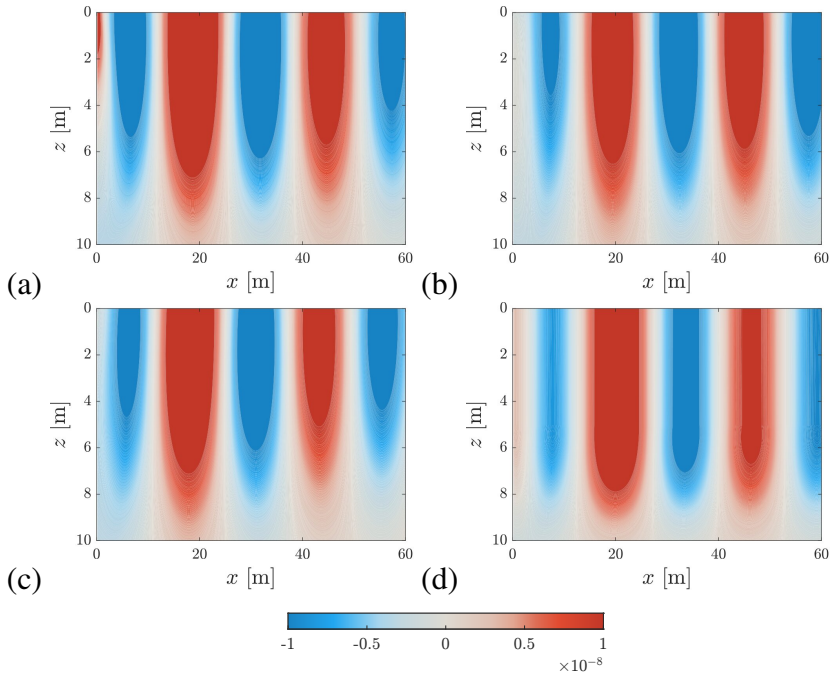

Figure 7: P-SV Green's displacement $\hat{u}^{\mathrm{G}}_{zz}(x_{\mathrm{s}}, z_{\mathrm{s}}, x, z)$ computed at $f = 5\,\mathrm{Hz}$ for an out-of-plane concentrated load applied at $x_{\mathrm{s}} = 0\,\mathrm{m}$ and $z_{\mathrm{s}} = 0\,\mathrm{m}$ using (a) FOM, (b) PGD, (c) GTA and (d) GHTA.

Table 2: Computational time comparison between reduced order algorithms and the FOM.

		SH [s]		P-SV [s]	
		(k_x, ω)	(x, ω)	(k_x, ω)	(x, ω)
FOM		0.62	1.81	0.850	2.800
PGD	offline	493.07	0.0324	546.6	0.061
	online	0.0031	0.0012	0.005	0.004
GTA	offline	855.20	0.0032	2427	0.061
	online	2.5581	2.5021	1.056	1.272
GHTA	offline	603.64	0.0324	942.6	0.061
	online	0.0432	0.0192	0.004	0.003

The corresponding storage requirements are summarized in table 3. The comparison demonstrates the reduced memory footprint of the low-rank tensor formats. PGD stores the solution as a sum of rank-one contributions, GTA stores the reduced basis matrices together with a global Tucker core and GHTA replaces this global core by hierarchical Tucker cores. The results demonstrate the compression capability of the reduced order representations relative to the full order Green's tensor.

The accuracy of the reduced order approximations is assessed through a relative Frobenius error computed from the Green's function response in the wavenumber-frequency domain. For

Table 3: Storage requirement comparison between reduced order algorithms and the FOM.

	SH [MB]		P-SV [MB]	
	(k_x, ω)	(x, ω)	(k_x, ω)	(x, ω)
FOM	366.2	161.1	552.9	92.16
PGD	0.367	0.184	0.404	0.209
GTA	1.139	0.956	1.404	1.209
GHTA	0.521	0.399	0.583	0.460

a reduced approximation obtained with rank or enrichment level $\mathbf{r}$, the error is defined as:

$$\varepsilon_{\mathbf{r}} = \frac{\left\| \tilde{\mathbf{u}}^{\mathrm{G}}_{\mathrm{FOM}} - \tilde{\mathbf{u}}^{\mathrm{G}}_{\mathrm{ROM}(\mathbf{r})} \right\|_{\mathrm{F}}}{\left\| \tilde{\mathbf{u}}^{\mathrm{G}}_{\mathrm{FOM}} \right\|_{\mathrm{F}}} \tag{16}$$

where $\tilde{\mathbf{u}}^{\mathrm{G}}_{\mathrm{FOM}}$ denotes the full order Green's tensor and $\tilde{\mathbf{u}}^{\mathrm{G}}_{\mathrm{ROM}(\mathbf{r})}$ denotes the reduced order approximation obtained for a prescribed rank or enrichment level $\mathbf{r}$. The parameter $\mathbf{r}$ denotes the retained approximation level used to construct the reduced representation. Its precise interpretation depends on the tensor format. The error $\varepsilon_{\mathbf{r}}$ is evaluated for a sequence of increasing ranks, ranging from one up to the prescribed maximum number of retained modes.

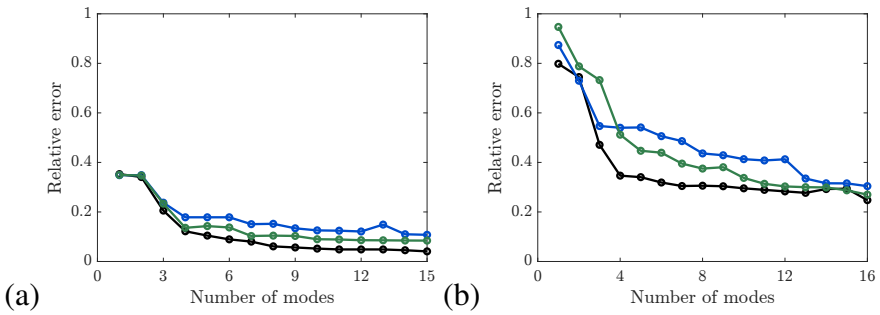

Figure 8: Relative Frobenius error of the reduced order approximations, PGD (blue), GTA (black) and GHTA (green) as a function of the rank for (a) SH and (b) P-SV problem.

Figure 8 shows the relative Frobenius error as a function of the retained rank. For the SH Green's function, the error decreases with increasing rank for all three reduced order approximations, although with different convergence rates. GTA gives the lowest error over the full range of ranks and reaches a final error of approximately 4%. The P-SV problem is more challenging due to the coupled compressional-shear response. For this case, the GTA approximation reaches an error level of approximately 25%, but further rank enrichment is limited by the growth of the Tucker core and the associated memory requirements. PGD shows the slowest reduction of the error, indicating that a larger number of rank-one terms is required to approximate the coupled response. The GHTA approximation follows an intermediate convergence trend. This is consistent with its hierarchical representation, the internal ranks allow coupling within selected groups of variables, while limiting the size of the global coupling compared with the full Tucker core. For the rank settings used here, GHTA error remains between the PGD and GTA errors, however, the target error level of 1-2% has not yet been achieved. The accuracy of GHTA is influenced by the selected dimension tree and internal hierarchical ranks. Increasing these ranks improves the

approximation by allowing stronger coupling between grouped variables, but it also increases the size of the hierarchical cores and the corresponding computational cost. Moreover, if the additional hierarchical directions are weakly independent, the hierarchical core least-squares problem tends to become ill-conditioned. The present results therefore indicate that GHTA provides a tunable representation between the compact but restrictive PGD format and the more accurate but less scalable Tucker format. This makes the choice of internal ranks and dimension tree central to balancing accuracy, storage, computational efficiency and numerical robustness.

5 CONCLUSIONS

This study highlights the potential of greedy low-rank tensor approximations for reducing the computational and storage demands associated with multidimensional elastodynamic Green's functions. By representing the Green's function over source, receiver and spectral variables in separated tensor form, the response can be stored and evaluated more efficiently than with a direct full order representation.

A central issue remains the extension of low-rank Green's function approximations to larger parametric settings. While Tucker-based approximations provide an effective coupling of the reduced spaces, the size of the core tensor grows with the product of the ranks in all separated directions. This can become restrictive when additional variables, such as frequency, material properties, layer parameters, or multiple spatial coordinates, are included simultaneously. The hierarchical Tucker formulation offers a way to mitigate this limitation by replacing the single global core with a hierarchy of smaller coupling tensors, allowing the multidimensional structure to be represented in a more scalable form. The results presented in the paper provide a proof of concept that GHTA can provide an intermediate representation between fully separable and full Tucker formats, with its accuracy and efficiency governed by the selected dimension tree and internal hierarchical ranks. This makes the method a useful candidate for exploring more scalable Green's function representations, although its performance remains problem-dependent and sensitive to rank selection and numerical conditioning.

Future work will focus on adaptive selection of dimension trees and hierarchical ranks, improved conditioning of the hierarchical core solves and extension of the formulation to broader parametric studies involving frequency variation, material properties and more general layered configurations relevant to wave propagation and soil-structure interaction analyses.

References

[1] A. Bedford and D. S. Drumheller. *Introduction to Elastic Wave Propagation*. 2nd. Springer, 2017.

[2] A. K. Chopra. *Dynamics of Structures: Theory and Applications to Earthquake Engineering*. 4th. Pearson, 2012.

[3] M. Bonnet. *Boundary integral equation methods for solids and fluids*. Chichester, United Kingdom: John Wiley and Sons, 1995.

[4] P. Benner et al. *Model Reduction and Approximation*. Society for Industrial and Applied Mathematics, 2017.

[5] V. Pereyra and B. Kaelin. "Fast wave propagation by model order reduction". In: *Electronic Transactions on Numerical Analysis* 30 (2008), pp. 406–419.

[6] J. M. Rekoske, D. A. May, and A. A. Gabriel. "Reduced-order modelling for complex three-dimensional seismic wave propagation". In: *Geophysical Journal International* 241 (2025), pp. 526–548.

[7] B. Besselink et al. "A comparison of model reduction techniques from structural dynamics, numerical mathematics and systems and control". In: *Journal of Sound and Vibration* 332 (2013), pp. 4403–4422.

[8] K. Lu et al. "A Review of Model Order Reduction Methods for Large-Scale Structure Systems". In: *Shock and Vibration* 2021.1 (2021), p. 6631180.

[9] H. Luo et al. "A multi-scale model-order reduction strategy for vibration analysis of coupled structures with local inhomogeneities". In: *Computers and Structures* 290 (2024), p. 107191.

[10] P. Benner, S. Gugercin, and K. Willcox. "A Survey of Projection-Based Model Reduction Methods for Parametric Dynamical Systems". In: *SIAM Review* 57.4 (2015), pp. 483–531.

[11] H. A. Jensen et al. "An effective parametric model reduction technique for uncertainty propagation analysis in structural dynamics". In: *Reliability Engineering and System Safety* 195 (2020), p. 106723.

[12] Y. Kim et al. "Parametric reduced-order modeling enhancement for a geometrically imperfect component via hyper-reduction". In: *Computer Methods in Applied Mechanics and Engineering* 403 (2023), p. 115701.

[13] R. Othman, A. Ammar, and K. Almitani. "Reduced modelling computation of layered soil's harmonic green functions". In: *Finite Elements in Analysis and Design* 177 (2020), p. 103419.

[14] F. Chinesta, R. Keunings, and A. Leygue. *The Proper Generalized Decomposition for Advanced Numerical Simulations: a Primer*. Springer, 2013.

[15] A. Nouy. "A priori model reduction through Proper Generalized Decomposition for solving time-dependent partial differential equations". In: *Computer Methods in Applied Mechanics and Engineering* 199 (2010), pp. 1603–1626.

[16] I. Georgieva and C. Hofreither. "Greedy low-rank approximation in Tucker format of solutions of tensor linear systems". In: *Journal of Computational and Applied Mathematics* 358 (2019), pp. 206–220.

[17] T. Kolda and B. Bader. "Tensor Decompositions and Applications". In: *SIAM Review* 51 (2009), pp. 455–500.

[18] Z. Farooq et al. *Reduced order computation of 2D elastodynamic Green's functions in layered soil using a low-rank tensor approximation*. 2026. DOI: 10.48550/arXiv.2603.19080. arXiv: 2603.19080 [math.NA].

[19] D. Kressner and C. Tobler. "Algorithm 941: htucker—A Matlab Toolbox for Tensors in Hierarchical Tucker Format". In: *ACM Transactions on Mathematical Software* 40.3 (2014).

[20] E. Kausel and J. Roësset. "Stiffness matrices for layered soils". In: *Bulletin of the Seismological Society of America* 71.6 (1981), pp. 1743–1761.

[21] F. Molenkamp and I. Smith. "Hysteretic and viscous material damping". In: *International Journal for Numerical and Analytical Methods in Geomechanics* 4 (1980), pp. 293–311.

[22] M. Schevenels, S. François, and G. Degrande. “EDT: An ElastoDynamics Toolbox for MATLAB”. In: *Computers & Geosciences* 35 (2009), pp. 1752–1754.

[23] J. Talman. “Numerical Fourier and Bessel transforms in logarithmic variables”. In: *Journal of Computational Physics* 29.1 (1978), pp. 35–48.

[24] I. Viktorov. *Rayleigh and Lamb waves: physical theory and applications*. New York, NY: Plenum Press, 1967.